Inorg. Chem. **2006**, *45*, 5552–5560

Luminescent Amidate-Bridged One-Dimensional Platinum(II)–Thallium(I) Coordination Polymers Assembled via Metallophilic Attraction

Wanzhi Chen,*,† Fenghui Liu,† Duanjun Xu,† Kazuko Matsumoto,*,‡ Shinobu Kishi,§ and Masako Kato§

Department of Chemistry, Zhejiang University, Hangzhou 310028, P. R. China, and Department of Chemistry, Advanced Research Institute for Science and Engineering, Waseda University, Okubo, Shinjuku ku 169-8555, Japan, and Division of Material Science, Graduate School of Human Culture, Nara Women's University, Nara 630-8506, Japan

Received November 8, 2005

The neutral square-planar complexes $[Pt(RNH_2)_2(NHCO^tBu)_2]$ (R = H, **1**; Et, **2**) and $[Pt(DACH)(NHCO^tBu)_2]$ (DACH = 1,2-diaminocyclohexane, **3**) act as metalloligands and make bonds to closed-shell Tl(I) ions to afford one- and two-dimensional platinum–thallium oligomers or polymers based on heterobimetallic backbones. A series of heteronuclear platinum(II)–thallium(I) complexes have been synthesized and structurally characterized. The structures of the Pt–Tl compounds resulted from $[Pt(RNH_2)_2(NHCO^tBu)_2]$ and TlX [X = NO_3^-, ClO_4^-, PF_6^-, and $Cp_2Fe(CO_2)_2^{2-}$] are dependent on both counteranions and the amine substituents. The compounds $[Pt(NH_3)_2(NHCO^tBu)_2Tl]X$ (X = NO_3^-, **8**; ClO_4^-, **9**) adopt one-dimensional zigzag chain structures consisting of repeatedly stacked $[Pt(NH_3)_2(NHCO^tBu)_2Tl]^+$ units, whereas $[\{Pt(NH_3)_2(NHCO^tBu)_2\}_2Tl_2]X_2$ (X = PF_6^-, **10**) consists of a helical chain. Compound **3** reacts with Tl^+ to give $[\{Pt(DACH)(NHCO^tBu)_2\}_2Tl](NO_3)\cdot[Pt(DACH)(NHCO^tBu)_2]\cdot 3H_2O$ (**14**) and one-dimensional polymeric $[\{Pt(DACH)(NHCO^tBu)_2\}_2Tl_2]X_2$ (X = ClO_4^-, **15**; PF_6^-, **16**). Reactions of $[Pt(DACH)(NHCOCH_3)_2]$ with Tl^+ ions afford one-dimensional coordination polymers $[\{Pt(DACH)(NHCOCH_3)_2\}_2Tl_2]X_2$ (X = NO_3^-, **17**; ClO_4^-, **18**; PF_6^-, **19**). The polymeric $[\{Pt(DACH)(NHCOR')_2\}_2Tl_2]^{2+}$ (R = CH_3, ^{t}Bu) complexes adopt helical structures, which are generated around the crystallographic 2_1 screw axis. The distance between the coils corresponds to the unit cell length, which ranges from 22.58 to 22.68 Å. The platinum–thallium bond distances fall in a narrow range around 3.0 Å. The complexes derived from $[Pt(NH_3)_2(NHCO^tBu)_2]$ are luminescent at 77 K. The trinuclear complexes $[\{Pt(RNH_2)(NHCO^tBu)_2\}_2Tl]^+$ do not emit at room temperature but are emissive at 77 K, whereas the polymeric platinum–thallium complexes containing 1,2-diaminocyclohexane are intensively luminescent at both room temperature and 77 K. The color variations are interesting; **15** exhibits intense yellow-green, **16** exhibits green, and **17**–**19** exhibit blue luminescence. The presence of bonding between platinum and thallium is supported by the short metal–metal separations and the strong low-energy luminescence of these compounds in their solid states.

Introduction

Electronic communication between atoms or atomic groups is a fundamental process to many complex chemical systems in biochemical and material sciences.[1] Direct electronic transfer processes between metal atoms are especially important because this phenomenon is often associated with many potentially useful chemical and physical properties of materials such as catalytic behavior, magnetic, optical, or electronic properties.[2] Metal−metal interactions between closed-shell heavy metals have recently been widely recognized and termed as *metallophilicity*.[3−7] Experimental and theoretical evidences have been accumulated for these interactions in recent years. The $d^8-d^{10}-s^2$ closed-shell metallophilic interactions and ligand functionality have resulted in the formation and isolation of multinuclear aggregates with novel and diverse structures.[8] Examples of

* Corresponding authors. Fax: 81 3-5273-3489 (K.M.). E-mail: chenwzz@zju.edu.cn (W.C.), kmatsu@waseda.jp (K.M.).
† Zhejiang University.
‡ Waseda University.
§ Nara Women's University.

(1) (a) Berg, A.; Shuali, Z.; Asano-Someda, M.; Levanon, H.; Fuhs, M.; Mobius, K.; Wang, R.; Brown, C.; Sessler J. L. *J. Am. Chem. Soc.* **1999**, *121*, 7433. (b) Pasternack, R. F.; Caccam, M.; Keogh, B.; Stephenson, T. A.; Williams, A. P.; Gibbs, E. J. *J. Am. Chem. Soc.* **1991**, *113*, 6835. (c) Seo, J.; Kim, S.; Park, S. Y. *J. Am. Chem. Soc.* **2004**, *126*, 11154. (d) Allis, D. G.; Spencer, J. T. *Inorg. Chem.* **2001**, *40*, 3373. (e) Xu, G.-L.; DeRosa, M. C.; Crutchley, R. J.; Ren, T. *J. Am. Chem. Soc.* **2004**, *126*, 3728.

10.1021/ic051932c CCC: $33.50
Published on Web 06/09/2006

heterobimetallic platinum−thallium complexes containing such a kind of interaction are seen in the literature for $Pt^{II}-Tl^{I}$,[4] $Pt^{II}-Tl^{II}$,[5] $Pt^{0}-Tl^{I}$,[6] and $Pt^{II}-Tl^{III}$ compounds.[7] One of the most intriguing features in the reported platinum−thallium complexes is the high tendency to make metal−metal interactions. Only a few $Pt^{II}-Tl^{I}$ complexes have been found to be emissive, and the luminescence is correlated with the metal aggregation through platinum−thallium interactions. The theoretical studies of the electronic structure of $Tl_2Pt(CN)_4$ showed that the metal−metal interaction involves a substantial σ orbital overlap between the 6s and $6p_z$ valence orbitals of Tl and the $5d_z^2$ and $6p_z$ valence orbitals of Pt.[9] Particularly interesting are extended linear metal−metal chain compounds, because the rationalization of the bonding in these structures still remains a challenge, and these compounds display fascinating and unique chemical and physical properties.[10]

It is well-recognized that weak interatomic interactions, such as hydrogen bonding and $\pi-\pi$ stacking, have presented a synthetic paradigm for the rational design and synthesis of functional materials in supramolecular chemistry.[11] Aurophilic interactions of an order-of-magnitude greater strength comparable to hydrogen bonds have been used as an element for the crystal engineering design of homo- and heterobimetallic coordination polymers.[12] Although metallophilic interactions between metals other than gold are weaker, the interaction can also be used to control the conformation and topology of heterometallic aggregates. However, in contrast to the many known coordination polymers containing $d^{10}-d^{10}$ interactions,[13] most Pt−Tl bonded complexes contain discrete Pt−Tl or Pt−Tl−Pt molecules, and the coordination polymers containing platinum−thallium d^8-s^2 metallophilic interactions have been only scarcely reported.[14]

We have been interested in the synthesis and reactivity of multinuclear complexes of platinum bearing amidate groups as the bridging ligands.[15,16] The neutral square-planar platinum complex $[Pt(RNH_2)_2(NHCO^tBu)_2]$ has proven to be a valuable precursor for the synthesis of a variety of homo- and heteronuclear complexes with the amidate ligand bridging the metal centers (see Chart 1).[16] The complex $[Pt(RNH_2)_2(NHCOR')_2]$ as a whole may be viewed as a potentially tetradentate metalloligand when the two oxygen

(2) (a) Campbell, K.; Kuehl, C. J.; Ferguson, M. J.; Stang P. J.; Tykwinski, R. R. *J. Am. Chem. Soc.* **2002**, *124*, 7266. (b) Papaefstathiou, G. S.; MacGillivray, L. R. *Angew. Chem., Int. Ed.* **2002**, *41*, 2070. (c) Noveron, J. C.; Lah, M. S.; Del Sesto, R. E.; Arif, A. M.; Miller, J. S.; Stang, P. J. *J. Am. Chem. Soc.* **2002**, *124*, 6613. (d) Stahl, J.; Bohling, J. C.; Bauer, E. B.; Peters, T. B.; Mohr, W.; Martin-Alvarez, J. M.; Hampel, F.; Gladysz, J. A. *Angew. Chem., Int. Ed.* **2002**, *41*, 1872. (e) Fernandez, E. J.; Jones, P. G.; Laguna, A.; Lopez-de-Luzuriaga, J. M.; Monge, M.; Perez, J.; Olmos, M. E. *Inorg. Chem.* **2002**, *41*, 1056.

(3) (a) Pyykkō, P. *Chem. Rev.* **1997**, *97*, 597. (b) Pyykkō, P. *Chem. Rev.* **1988**, *88*, 563. (c) White-Morris, R. L.; Olmstead, M. M.; Jiang, F.; Tinti, D. S.; Balch, A. L. *J. Am. Chem. Soc.* **2002**, *124*, 2327. (d) Olmstead, M. M.; Jiang, F.; Attar, S.; Balch, A. L. *J. Am. Chem. Soc.* **2001**, *123*, 3260. (e) Lu, W.; Xiang, H.; Zhu, N.; Che, C. *Organometallics* **2002**, *21*, 2345. (f) Leznoff, D. B.; Xue, B.; Batchelor, R. J.; Einstein, F. W. B.; Patrick, B. O. *Inorg. Chem.* **2001**, *40*, 6026. (g) Fernandez, E. J.; Lopez-de-Luzuriaga, J. M.; Monge, M.; Olmos, M. E.; Perez, J.; Laguna, A. *J. Am. Chem. Soc.* **2002**, *124*, 5942.

(4) (a) Nagle, J. K.; Balch, A. L.; Olmstead, M. M. *J. Am. Chem. Soc.* **1988**, *110*, 319. (b) Usón, R.; Forniés, J.; Tomas, M.; Garde, R.; Alonso, P. *J. Am. Chem. Soc.* **1995**, *117*, 1837. (c) Berenguer, J. R.; Forniés, J.; Gómez, J.; Lalinde, E.; Moreno, M. T. *Organometallics* **2001**, *20*, 4847−4851. (d) Ezomo, O. J.; Mingos, D. M. P.; Williams, I. D. *J. Chem. Soc., Chem. Commun.* **1987**, 924. (e) Renn, O.; Lippert, B.; Mutikainen, I. *Inorg. Chim. Acta* **1993**, *208*, 219. (f) Usón, R.; Forniés, J.; Tomás, M.; Garde, R.; Merino, R. I. *Inorg. Chem.* **1997**, *36*, 1383. (g) Omary, M. A.; Webb, T. R.; Assefa, Z.; Shankle, G. E.; Patterson, H. H. *Inorg. Chem.* **1998**, *37*, 1380. (h) Balch, A. L.; Rowley, S. P. *J. Am. Chem. Soc.* **1990**, *112*, 6139. (i) Ara, I.; Berenguer, J. R.; Fornies, J.; Gomez, J.; Lalinde, E.; Merino, R. I. *Inorg. Chem.* **1997**, *36*, 6461. (j) Charmant, J. P. H.; Fornies, J.; Gomez, J.; Lalinde, E.; Merino, R. I.; Moreno, M. T.; Orpen, A. G. *Organometallics* **2003**, *22*, 652. (k) Song, H.-B.; Zhang, Z.-Z.; Hui, Z.; Che, C.-M.; Mak, T. C. W. *Inorg. Chem.* **2002**, *41*, 3146. (l) Stork, J. R.; Olmstead, M. M.; Balch, A. L. *J. Am. Chem. Soc.* **2005**, *127*, 6512.

(5) Usón, R.; Forniés, J.; Tomás, M.; Garde, R. *J. Am. Chem. Soc.* **1995**, *117*, 1837.

(6) (a) Catalano, V. J.; Bennett, B. L.; Yson, R. L.; Noll, B. C. *J. Am. Chem. Soc.* **2000**, *122*, 10056. (b) Catalano, V. J.; Bennett, B. L.; Muratidis, S.; Noll, B. C. *J. Am. Chem. Soc.* **2001**, *123*, 173. (c) Hao, L.; Xiao, J.; Vittal, J. J.; Puddephatt, R. J.; Manojlovic-Muir, L.; Muir, K. W.; Torai, A. A. *Inorg. Chem.* **1996**, *35*, 658. (d) Stadnichenko, R.; Sterenberg, B. T.; Bradford, A. M.; Jennings, M. C.; Puddephatt, R. J. *J. Chem. Soc., Dalton Trans.* **2002**, 1212−1216.

(7) (a) Maliarik, M.; Berg, K.; Glaser, K. J.; Sandström, M.; Tóth, I. *Inorg. Chem.* **1998**, *37*, 2910. (b) Berg, K.; Glaser, J.; Read, M. C.; Tóth, I. *J. Am. Chem. Soc.* **1995**, *117*, 7550. (c) Alilehvand, F.; Maliarik, J. M.; Sandström, M.; Mink, J.; Persson, I.; Persson, P.; Tóth, I.; Glaser, J. *Inorg. Chem.* **2001**, *40*, 3889. (d) Ma, G.; Kritikos, M.; Glaser, J. *Eur. J. Inorg. Chem.* **2001**, 1311. (e) Ma, G.; Molla-Abbassi, A.; Kritikos, M.; Ilyukhin, A.; Jalilehvand, F.; Kessler, V.; Skripkin, M.; Sandström, M.; Glaser, J.; Näslund, J.; Persson, I. *Inorg. Chem.* **2001**, *40*, 6432. (f) Catalano, V. J.; Malwitz, M. A. *J. Am. Chem. Soc.* **2004**, *126*, 6560.

(8) Enomoto, M.; Kishimura, A.; Aida, T. *J. Am. Chem. Soc.* **2001**, *123*, 5608. (b) Lee, Y.; Eisenberg, R. *J. Am. Chem. Soc.* **2003**, *125*, 7778. (c) Maspero, A.; Kani, I.; Mohamed, A. A.; Omary, M. A.; Staples, R. J.; Fackler, J. P., Jr. *Inorg. Chem.* **2003**, *42*, 5311. (c) Stender, M.; White-Morris, R. L.; Olmstead, M. M.; Balch, A. L. *Inorg. Chem.* **2003**, *42*, 4504.

(9) Ziegler, T.; Nagle, J. K.; Snijders, J. G.; Baerends, E. J. *J. Am. Chem. Soc.* **1989**, *111*, 5631.

(10) (a) Mitsumi, M.; Murase, T.; Kishida, H.; Yoshinari, T.; Ozawa, Y.; Toriumi, K.; Sonoyama, T.; Kitagawa, H.; Mitani, T. *J. Am. Chem. Soc.* **2001**, *123*, 11179. (b) Bremi, J.; Brovelli, D.; Caseri, W.; Hahner, G.; Smith, P.; Tervoort, T. *Chem. Mater.* **1999**, *11*, 977. (c) Buss, C. E.; Mann, K. R. *J. Am. Chem. Soc.* **2002**, *124*, 1031.

(11) (a) Mak, T. C. W.; Xue, F. *J. Am. Chem. Soc.* **2000**, *122*, 9860. (b) Shi, Z.; Li, Y.; Gong, H.; Liu, M.; Xiao, S.; Liu, H.; Li, H.; Xiao, S.; Zhu, D. *Org. Lett.* **2002**, *4*, 1179. (c) Gong, B.; Yan, Y.; Zeng, H.; Skrzypczak-Jankunn, E.; Kim, Y. W.; Zhu, J.; Ickes, H. *J. Am. Chem. Soc.* **1999**, *121*, 5607.

(12) (a) Colacio, E.; Lloret, F.; Kivekas, R.; Suarez-Varela, J.; Sundberg, M. R.; Uggla, R. *Inorg. Chem.* **2003**, *42*, 560−565. (b) Hunks, W. J.; Jennings, M. C.; Puddephatt, R. J. *Inorg. Chem.* **2002**, *41*, 4590.

(13) (a) Ehlich, H.; Schier, A.; Schmidbaur, H. *Inorg. Chem.* **2002**, *41*, 3721. (b) Assefa, Z.; Omary, M. A.; McBurnett, B. G.; Fackler, J. P., Jr.; Patterson, H. H.; Staples, R. J.; Mohamed, A. A. *Inorg. Chem.* **2002**, *41*, 6274. (c) Mohamed, A. A.; Burini, A.; Fackler, J. P., Jr. *J. Am. Chem. Soc.* **2005**, *127*, 5012. (d) Catalano, V. J.; Malwitz, M. A. *J. Am. Chem. Soc.* **2004**, *126*, 6560. (e) Schwerdtfeger, P.; Krawczyk, R. P.; Hammerl, A.; Brown, R. *Inorg. Chem.* **2004**, *43*, 6707. (f) Catalano, V. J.; Malwitz, M. A.; Etogo, A. O. *Inorg. Chem.* **2004**, *43*, 5714.

(14) (a) Ara, I.; Berenguar, J. R.; Forniés, J.; Gómez, J.; Lalinde, E.; Merino, R. I. *Inorg. Chem.* **1997**, *36*, 6461. (b) Stork, J. R.; Olmstead, M. M.; Balch, A. L. *J. Am. Chem. Soc.* **2005**, *127*, 6512.

(15) (a) Matsumoto, K.; Sakai, K. *Adv. Inorg. Chem.* **1999**, *49*, 375 and references therein. (b) Lin, Y.; Misawa, H.; Matsumoto, K. *J. Am. Chem. Soc.* **2001**, *123*, 569. (c) Matsumoto, K.; Matsunami, J.; Mizuno, K.; Uenura, H. *J. Am. Chem. Soc.* **1996**, *118*, 8959. (d) Lin, Y.; Takeda, S.; Matsumoto, K. *Organometallics* **1999**, *18*, 4897. (e) Chen, W.; Yamada, J.; Matsumoto, K.; *Synth. Commun.* **2002**, *32*, 17. (f) Matsumoto, K.; Nagai, Y.; Matsunami, J.; Mizuno, K.; Abe, T.; Somazawa, R.; Kinoshita, J.; Shimura, H. *J. Am. Chem. Soc.* **1998**, *120*, 2900.

(16) (a) Chen, W.; Matsumoto, K. *Inorg. Chim. Acta* **2003**, *342*, 88. (b) Chen, W.; Matsumoto, K. *Eur. J. Inorg. Chem.* **2002**, 2664. (c) Chen, W.; Liu, F.; Nishioka, T.; Matsumoto, K. *Eur. J. Inorg. Chem.* **2003**, 4234.

Chart 1

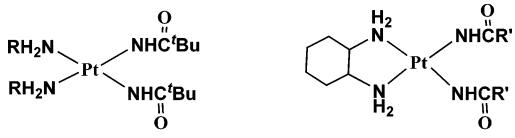

R = H (1), Et (2)

R' = ^{t}Bu (3), CH_3 (4)

atoms of the amidate ligands and the donor−acceptor ability of the platinum atom are considered. We describe herein the synthesis and X-ray single-crystal characterization of a new family of oligomeric and polymeric platinum−thallium complexes stabilized by amidate bridging ligands and platinum−thallium metallophilic interactions. Their spectroscopic and luminescent properties have also been studied. The polymeric complexes are very sparingly soluble in common solvents but soluble in DMSO with fragmentation to smaller units. Structural characterization of these complexes therefore relies primarily on X-ray diffraction analysis in their solid state.

Experimental Section

Materials and Physical Measurements. Compounds $[Pt(RNH_2)_2(NC^tBu)_2](ClO_4)_2$ and $[Pt(RNH_2)_2(NHCO^tBu)_2]$ (RNH_2 = NH_3, $EtNH_2$, and 1,2-diaminocyclohexane) were prepared according to the reported procedure.[16a] Compounds $[Pt(DACH)Cl_2]$ and $[Pt(DACH)I_2]$ (DACH = 1,2-diaminocyclohexane) were synthesized by using the known method.[17] Other chemicals were purchased and used as received. Microanalyses (C, H, and N) were performed by using a Perkin-Elmer 2400II analyzer. The ^{1}H and ^{195}Pt NMR spectra were recorded on a Bruker 500 MHz spectrometer at ambient temperature, and the frequencies are referenced to the resonance of TMS (^{1}H) and K_2PtCl_4 (^{195}Pt). Emission spectra were recorded on a Hitachi 850 spectrofluorimeter and a Nikon P-250 spectrometer with a photomultiplier equipped with a liquid He cryostat (Oxford CF1204).

$[Pt(DACH)(NHCO^tBu)_2]\cdot 4H_2O$ (3). To a suspension of **5** (0.69 g, 1.0 mmol) in 10 mL of water was added an aqueous solution of NaOH (1 mol/L, 2.2 mL). The mixture was stirred overnight to afford a white solid, which was collected and washed with water and dried in the air. Yield: 0.55 g (96%). Anal. Calcd for $C_{16}H_{34}N_4O_2Pt\cdot 4H_2O$: C, 33.04; H, 7.28; N, 9.63. Found: C, 33.29; H, 6.78; N, 9.57. ^{1}H NMR (500 MHz, DMSO-d_6): 6.50 (d, J_{HH} = 9.0 Hz, NH_2, 2H), 5.47 (s, NH, 2H), 4.64 (pseudo t, J_{HH} = 9.0 Hz, NH_2, 2H), 2.21, 1.91, 1.52, 1.29, 1.10 (m, C_6H_{10}, 10H), 1.07 (s, CH_3, 18H). ^{195}Pt NMR (107.30, DMSO-d_6): −2625.

$[Pt(DACH)(NHCOCH_3)_2]$ (4). The compound was similarly prepared by starting from **6** and proceeding as described for **3**. Yield: 91%. Anal. Calcd for $C_{10}H_{22}N_4O_2Pt$: C, 28.23; H, 5.21; N, 13.17. Found: C, 27.89; H, 5.46; N, 13.01. ^{1}H NMR (500 MHz, DMSO-d_6): 6.40 (d, J_{HH} = 9.0 Hz, NH_2, 2H), 5.40 (s, NH, 2H), 4.64 (pseudo t, J_{HH} = 11 Hz, NH_2, 2H), 2.27, 1.89, 1.50, 1.29, 1.17 (m, C_6H_{10}, 10H), 1.76 (s, CH_3, 6H). ^{195}Pt NMR (107.30, DMSO-d_6): −2631.

$[Pt(DACH)(NC^tBu)_2](ClO_4)_2\cdot H_2O$ (5). A suspension of $Pt(DACH)Cl_2$ (0.76 g, 2.0 mmol) in 10 mL of water was treated with $AgClO_4$ (0.83 g, 4.0 mmol), and the mixture was stirred overnight in the dark. After the removal of AgCl, ^{t}BuCN (0.83 g, 10 mmol) was added to the filtrate. The resulting white precipitate was separated and washed with H_2O, EtOH, and Et_2O and dried in the air. Yield: 1.3 g (94%). Anal. Calcd for $C_{16}H_{32}Cl_2N_4O_8Pt\cdot H_2O$: C, 27.75; H, 4.95; N, 8.09. Found: C, 27.55; H, 4.93; N, 7.94. ^{1}H NMR (500 MHz, DMSO-d_6): 1.54 (s, CH_3, 18H), 2.75, 2.20, 1.56, 1.38, 1.20 (m, C_6H_{10}, 10H). ^{195}Pt NMR (107.30, acetone-d_6): −2857.

$[Pt(DACH)(NCCH_3)_2](ClO_4)_2$ (6). The compound was similarly prepared by starting from $Pt(DACH)Cl_2$, $AgClO_4$, and CH_3CN and proceeding as described for **5**. Yield: 93%. Anal. Calcd for $C_{10}H_{20}Cl_2N_4O_8Pt$: C, 20.35; H, 3.42; N, 9.49. Found: C, 20.03; H, 3.69; N, 9.10. ^{1}H NMR (500 MHz, DMSO-d_6): 2.60 (s, CH_3, 6H), 2.52, 2.11, 1.56, 1.38, 1.14 (m, C_6H_{10}, 10H). ^{195}Pt NMR (107.30, DMSO-d_6): −2864.

[1,1′-Fe(CpCO$_2$Tl)$_2$] (7). To a solution of $TlNO_3$ (53 mg, 0.2 mmol) in 5 mL of H_2O was added disodium 1,1′-ferrocenyldicarboxylate (0.32 mg, 0.1 mmol). A red precipitate was immediately isolated, which was washed with water and dried in the air. Yield: 65 mg (95%). Anal. Calcd for $C_{12}H_8O_4FeTl_2$: C, 21.17; H, 1.18. Found: C, 20.84; H, 0.92.

$[Pt(NH_3)_2(NHCO^tBu)_2Tl](NO_3)$ (8). To a solution of $TlNO_3$ (26.6 mg, 0.1 mmol) in 2 mL of water was added $[Pt(NH_3)_2(NHCO^tBu)_2]\cdot 2H_2O$ (46.5 mg, 0.1 mmol), and the mixture was stirred for 10 min. To the mixture was added 2 mL of acetone. Slow evaporation of the resulted colorless solution yielded yellow crystals. Collection and drying in a vacuum gave a yellow solid (54.2 mg, 78%). Anal. Calcd for $C_{10}H_{26}N_5O_5PtTl$: C, 17.26; H, 3.77; N, 10.07. Found: C, 17.32; H, 3.64; N, 10.01. ^{1}H NMR (500 MHz, DMSO-d_6): δ 5.03 (s, NH, 2H), 4.22 (s, NH_3, 6H), 1.03 (s, CH_3, 18H).

$[Pt(NH_3)_2(NHCO^tBu)_2Tl](ClO_4)$ (9). The complex was prepared in a manner identical to that for **8** in the presence of $NaClO_4$ (50 mg). Slow evaporation of the solvent gave **9** as yellow crystalline solid (59.3 mg, 81%). Anal. Calcd for $C_{10}H_{26}ClN_4O_6PtTl$: C, 16.38; H, 3.57; N, 7.64. Found: C, 15.91; H, 3.52; N, 7.32. ^{1}H NMR (500 MHz, DMSO-d_6): δ 4.99 (s, NH, 2H), 4.23 (s, NH_3, 6H), 1.03 (s, CH_3, 18H). ^{195}Pt NMR (107.3 MHz, DMSO-d_6): δ −2135.9.

$[\{Pt(NH_3)_2(NHCO^tBu)\}_2Tl_2](PF_6)_2\cdot(CH_3)_2CO\cdot H_2O$ (10). The complex was prepared in a manner identical to that for **8** in the presence of $NaPF_6$ (50 mg). Slow evaporation of the solvent gave **12** as yellow-green crystalline solid (62 mg, 76%). Anal. Calcd for $C_{20}H_{52}F_{12}N_8O_4P_2Pt_2Tl_2\cdot(CH_3)_2CO\cdot H_2O$: C, 16.91; H, 3.70; N, 6.86. Found: C, 17.35; H, 3.56; N, 6.83. ^{1}H NMR (500 MHz, DMSO-d_6): δ 5.06 (s, NH, 4H), 4.18 (s, NH_3, 12H), 2.07[s, $(CH_3)_2CO$, 6H], 1.03 (s, CH_3, 36H). ^{195}Pt NMR (107.3 MHz, DMSO-d_6): δ −2134.2.

$[\{Pt(NH_3)_2(NHCO^tBu)\}_2Tl_2](NO_3)_2\cdot EtOH\cdot H_2O$ (11). A solution of $TlNO_3$ (26.6 mg, 0.1 mmol) and $[Pt(NH_3)_2(NHCO^tBu)_2]\cdot 2H_2O$ (46.5 mg, 0.1 mmol) in 2 mL of water was heated at 50 °C for 10 min. Slow evaporation of the resulted colorless solution yielded yellow crystals (62 mg, 86%). Anal. Calcd for $C_{20}H_{52}N_{10}O_{10}Pt_2Tl_2$: C, 17.56; H, 4.12; N, 9.97. Found: C, 17.26; H, 3.77; N, 10.07.

$[\{Pt(NH_3)_2(NHCO^tBu)\}_2Tl_2](PF_6)_2\cdot 2(CH_3)_2CO$ (12). An aqueous solution of $TlNO_3$ (26.6 mg, 0.1 mmol) and $[Pt(NH_3)_2(NHCO^tBu)_2]\cdot 2H_2O$ (46.5 mg, 0.1 mmol) and $NaPF_6$ (50 mg) in 2 mL of water were added to a solution of 4,4′-bipyridine (16 mg, 0.1 mmol) in 2 mL of acetone. The solution was allowed to evaporate slowly, and yellow crystals of **12** were afforded. Yield: (82%). Anal. Calcd for $C_{20}H_{52}F_{12}N_8O_4P_2Pt_2Tl_2\cdot 2(CH_3)_2CO$: C, 18.65; H, 3.85; N, 6.70. Found: C, 18.25; H, 3.56; N, 6.53.

$[\{Pt(EtNH_2)_2(NHCO^tBu)_2\}_2Tl](PF_6)\cdot H_2O$ (13). $[Pt(EtNH_2)_2(NHCO^tBu)_2]$ (48 mg, 0.1 mmol) was added to a mixture of $TlNO_3$

(17) Talebian, A. H.; Bensely, D.; Ghiorghis, A.; Hammer, C. F.; Schein, P. S.; Green, D. *Inorg. Chim. Acta* **1991**, *179*, 281.

Table 1. Crystallographic Data for Compounds **8**, **10**, **13**, **15**, and **20**[a]

	8	**10**	**13**	**15**	**20**
formula	$C_{10}H_{26}N_5O_5PtTl$	$C_{23}H_{60}F_{12}N_8O_6P_2Pt_2Tl_2$	$C_{28}H_{70}F_6N_8O_5PPt_2Tl$	$C_{33}H_{71}Cl_2N_8O_{12.5}Pt_2Tl_2$	$C_{44}H_{84}FeN_8O_{12}Pt_2Tl_2$
mol wt	695.82	1633.65	1338.44	1649.80	1826.01
cryst syst	monoclinic	trigonal	monoclinic	monoclinic	monoclinic
space group	$P2_1/c$	$P3_1$	$P2_1/c$	$P2_1$	$P2_1$
a, Å	17.130(5)	11.397(2)	13.872(7)	11.340(4)	11.830(7)
b, Å	10.123(3)	11.397(2)	20.352(10)	18.197(7)	21.660(12)
c, Å	11.669(4)	30.955(9)	17.305(9)	12.859(5)	12.683(7)
β,°	101.743(7)		96.395(9)	100.336(7)	103.340(10)
V, Å^3	1981.1(11)	3482.3(6)	4855(4)	2610.5(18)	3162(3)
Z	4	3	4	2	2
D_{calcd}, Mg/m^3	2.333	2.337	1.831	2.099	1.918
reflns collected	10390	19933	27680	15053	16717
reflns unique (R_{int})	3874 (0.0832)	7981 (0.0592)	10036 (0.0888)	9848 (0.0750)	10669 (0.1121)
R1, wR2 [$I > \sigma 2(I)$]	0.0410, 0.0698	0.0304, 0.0645	0.0453, 0.1041	0.0371, 0.0939	0.0690, 0.1507

[a] $R1 = \sum||F_o| - |F_c||/\sum|F_o|$. $wR2 = \{\sum[w(F_o^2 - F_c^2)^2]/\sum[w(F_o^2)^2]\}^{1/2}$.

(27 mg, 0.1 mmol) and NH_4PF_6 (50 mg) in 4 mL of water. Colorless crystals were grown after a few days. Yield: 61 mg (92%). Anal. Calcd for $C_{28}H_{68}F_6N_8O_4PPt_2Tl$: C, 25.47; H, 5.19; N, 8.49. Found: C, 25.30; H, 5.67; N, 8.52.

[{Pt(DACH)(NHCO^{t}Bu)(NHCO^{t}Bu)}$_2$Tl](NO$_3$)·[Pt(DACH)-(NHCO^{t}Bu)$_2$]·3H$_2$O (14). A solution of **3** (58 mg, 0.1 mmol) in 2 mL of acetone was added to an aqueous solution of $TlNO_3$ (26.6 mg, 0.1 mmol) in 4 mL of water. Colorless crystals of **14** were obtained upon slow evaporation of the resulted colorless solution. Yield: 47.4 mg (77%). Anal. Calcd for $C_{48}H_{102}N_{13}O_9Pt_3Tl·3H_2O$: C, 31.18; H, 5.89; N, 9.85. Found: C, 31.07; H, 5.77; N, 9.76. ^{1}H NMR (500 MHz, DMSO-d_6): 6.28 (d, $J_{HH} = 8.0$ Hz, NH_2, 6H), 5.21 (s, NH, 6H), 5.21 (pseudo t, $J_{HH} = 9.0$ Hz, NH_2, 6H), 2.23, 1.91, 1.49, 1.26, 1.09 (m, C_6H_{10}, 30H), 1.02 [s, $C(CH_3)_3$, 54H].

[{Pt(DACH)(NHCO^{t}Bu)$_2$}$_2$Tl$_2$](ClO$_4$)$_2$ (15). A solution of **3** (58 mg, 0.1 mmol) in 2 mL of acetone was added to an aqueous solution of $TlNO_3$ (26.6 mg, 0.10 mmol) and $NaClO_4$ (50 mg) in 2 mL of water. Yellow crystals of **15** were obtained upon slow evaporation of the resulted colorless solution. Yield: 65 mg (80%). Anal. Calcd for $C_{32}H_{68}Cl_2N_8O_{12}Pt_2Tl_2$: C, 23.63; H, 4.21; N, 6.89. Found: C, 23.63; H, 3.95; N, 6.70. ^{1}H NMR (500 MHz, DMSO-d_6): 5.94 (d, $J_{HH} = 9.0$ Hz, NH_2, 4H), 5.08 (t, NH_2, $J_{HH} = 8.5$ Hz, 4H), 5.03 (s, NH, 4H), 2.21, 1.98, 1.56, 1.29, 1.10 (m, C_6H_{10}, 10H), 1.06 [s, $C(CH_3)_3$, 36H]. ^{195}Pt NMR (107.30 MHz, DMSO-d_6): −2319.8.

[{Pt(DACH)(NHCO^{t}Bu)$_2$}$_2$Tl$_2$](PF$_6$)$_2$ (16). A solution of **3** (58 mg, 0.1 mmol) in 2 mL of acetone was added to an aqueous solution of $TlNO_3$ (26.6 mg, 0.10 mmol) and $NaPF_6$ (50 mg) in 2 mL of water. Yellow crystals of **16** were obtained upon slow evaporation of the resulted colorless solution. Yield: 74 mg (86%). Anal. Calcd for $C_{32}H_{68}F_{12}N_8O_4P_2Pt_2Tl_2$: C, 22.37; H, 3.99; N, 6.52. Found: C, 22.33; H, 3.89; N, 6.46. ^{1}H NMR (500 MHz, DMSO-d_6): 5.78 (s, NH, 4H), 5.04 (s, NH_2, 8H), 2.19, 1.92, 1.50, 1.24, 1.08 (m, C_6H_{10}, 20H), 1.04 [s, $C(CH_3)_3$, 36H].

[{Pt(DACH)(NHCOCH$_3$)$_2$}$_2$Tl$_2$](NO$_3$)$_2$·H$_2$O (17). Treatment of a solution of **4** (43 mg, 0.1 mmol) in 1 mL of H_2O with $TlNO_3$ (26.6 mg, 0.1 mmol) yielded a yellow precipitate. The addition of 1 mL of EtOH afforded a colorless solution. Yellow crystals suitable for X-ray diffraction analysis were obtained upon slow evaporation of the solution at room temperature. Yield: 56.7 mg (82%). Anal. Calcd for $C_{20}H_{44}N_{10}O_{10}Pt_2Tl_2$: C, 17.36; H, 3.21; N, 10.12. Found: C, 17.21; H, 3.38; N, 10.03. ^{1}H NMR (500 MHz, DMSO-d_6): 5.85, 5.35, 5.05 (br, NH + NH_2, 12H), 1.82 (s, CH_3, 12H), 2.32, 1.89, 1.51, 1.33, 1.02 (m, C_6H_{10}, 20H).

[{Pt(DACH)(NHCOCH$_3$)$_2$}$_2$Tl$_2$](ClO$_4$)$_2$ (18). The compound was obtained similarly as for **17** by adding an excess of $NaClO_4$. Yield: 64 mg (88%). Anal. Calcd for $C_{20}H_{44}Cl_2N_8O_{12}Pt_2Tl_2$: C, 16.47; H, 3.04; N, 7.68. Found: C, 16.45; H, 3.39; N, 7.43. ^{1}H NMR (500 MHz, DMSO-d_6): 5.35, 5.05 (br, NH + NH_2, 12H), 1.82 (s, CH_3, 12H), 2.32, 1.89, 1.51, 1.33, 1.02 (m, C_6H_{10}, 20H).

[{Pt(DACH)(NHCOCH$_3$)$_2$}$_2$Tl$_2$](PF$_6$)$_2$ (19). The compound was obtained similarly as for **18** by adding an excess of $NaPF_6$. Yield: 67 mg (86%). Anal. Calcd for $C_{20}H_{44}N_8O_4P_2F_{12}Pt_2Tl_2$: C, 15.50; H, 2.86; N, 7.23. Found: C, 22.15; H, 2.92; N, 6.96. ^{1}H NMR (500 MHz, DMSO-d_6): 5.34, 5.04 (br, NH + NH_2, 12H), 1.82 (s, CH_3, 12H), 2.32, 1.89, 1.51, 1.33, 1.02 (m, C_6H_{10}, 20H).

[{Pt(DACH)(NHCO^{t}Bu)$_2$}$_2${Fe(CpCO$_2$Tl)$_2$}] (20). A solution of **3** (58 mg, 0.1 mmol) in 2 mL of acetone was added to a suspension of [1,1′-$Cp_2Fe(CO_2Tl)_2$] (34 mg, 0.05 mmol). After stirring for 1 h, the resulted red solution was filtered. Red crystals suitable for X-ray diffraction analysis were isolated after slow evaporation of the solution. Yield: 45 mg (51%). Anal. Calcd for $C_{44}H_{84}FeN_8O_{12}Pt_2Tl_2$: C, 29.82; H, 4.78; N, 6.32. Found: C, 30.14; H, 4.64; N, 6.09.

X-ray Crystallography and Data Collection. The crystals were covered with inert oil and mounted on glass fibers. X-ray intensity data were collected on a Bruker Smart-*CCD* 1000 diffractometer equipped with Mo Kα radiation ($\lambda = 0.710\,73$ Å). The first 50 frames were recollected at the end of the process to monitor crystal decay. The raw frame data were integrated into *SHELX*-format reflection files and corrected for Lorentz and polarization effects by using *SAINT*.[18] All structures were solved by direct methods using SHELXS-97 and refined against F^2 by the full-matrix least-squares techniques with SHELXL-97.[19] All non-hydrogen atoms were refined anisotropically. The C−hydrogen atoms were introduced in their calculated positions. The absolute configurations of compounds that crystallize in noncentrosymmetric space groups were determined by refinement of the Flack x parameters. Crystallographic data for compounds **8**, **10**, **13**, **15**, and **20** are listed in Table 1, and those of compounds **9**, **11**, **12**, **14**, **16**, and **17** are given as Supporting Information.

Results and Discussion

Reactions of [Pt(NH$_3$)$_2$(NHCO^{t}Bu)$_2$]·2H$_2$O and Tl$^+$. Compound **8** was prepared in H_2O and acetone by mixing $TlNO_3$ and $[Pt(NH_3)_2(NHCO^tBu)_2]·2H_2O$ at a 1:1 molar ratio. Compounds **9** and **10** were obtained analogously in the presence of an excess of $NaClO_4$ or $NaPF_6$, respectively, as yellow and yellow-green crystals. Despite crystallizing in

(18) Sheldrick, G. M. *SHELXS-97*, Program for X-ray Crystal Structure Solution; University of Götingen: Götingen, Germany, 1997.
(19) Sheldrick, G. M. *SHELXL-97*, Program for X-ray Crystal Structure Refinement; University of Götingen: Götingen, Germany, 1997.

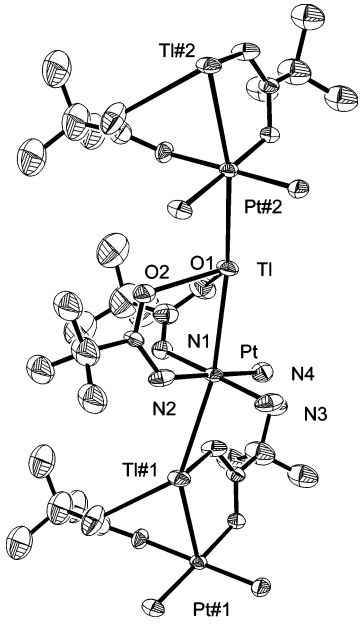

Figure 1. ORTEP drawing of the extended zigzag chain structure of $[Pt(NH_3)_2(NHCO^tBu)_2Tl]^+$ (**8**). Selected bond distances (Å) and angles (deg): Pt−Tl 2.921(1), Pt−Tl#1 3.115(1), Tl−Pt−Tl#1 172.85(3), Pt−Tl−Pt#2 150.36(2). Symmetry transformations used to generate equivalent atoms: #1 $x, -y + {}^1/_2, z - {}^1/_2$; #2 $x, -y + {}^1/_2, z + {}^1/_2$.

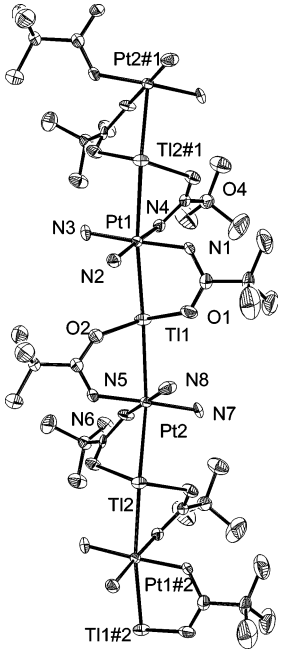

Figure 2. ORTEP drawing of the extended helical chain structure of $[\{Pt(NH_3)_2(NHCO^tBu)\}_2Tl_2]^{2+}$ (**10**). Selected bond distances (Å) and angles (deg): Pt1−Tl1 2.986(1), Pt1−Tl2#1 3.024(1), Pt2−Tl1 2.961(1), Pt2−Tl2 3.015(1), Pt2−Tl1−Pt1 143.08(2), Pt2−Tl2−Pt1#2 147.13(2), Tl1−Pt1−Tl2#1 169.73(2), Tl1−Pt2−Tl2 172.16(2). Symmetry code: #1 $x, y - 1, z$; #2 $x, y + 1, z$.

different space groups, compounds **8** and **9** display an identical supramolecular motif consisting of infinite zigzag chains. The structure of **8** is shown in Figure 1. The chains are comprised of an alternate stack of $[Pt(NH_3)_2(NHCO^tBu)_2]$ and Tl(I) ions. Thus, the thallium atoms sit above and below the square-planar $[Pt(NH_3)_2(NHCO^tBu)_2]$ units, completing an octahedron-like geometry around the platinum atom. The Pt−Tl bonds are approximately perpendicular to the Pt coordination planes. The Pt−Tl bond distances are 2.921(1) and 3.115(1) Å corresponding to the bridged Pt−Tl and unsupported Pt−Tl bonds, respectively, comparable to the sum of the metallic radii of platinum and thallium (3.08 Å). The "short" and "long" Pt−Tl bonds exhibit a zigzag arrangement with the Pt−Tl−Pt angle of 150.36(2)° and the Tl−Pt−Tl angle of 172.85(3)°. The Tl atom is unsymmetrically bonded to two oxygen atoms of the same $[Pt(NH_3)_2(NHCO^tBu)_2]$ unit. Compound **8** can be best viewed as an aggregation of the dimeric $[Pt(NH_3)_2(NHCO^tBu)_2Tl]^+$ unit via Pt−Tl metallophilic interactions. The Pt−Tl bond distances are usually 2.79−3.05 Å for Pt^0-Tl^I,[6] 2.81−3.14 Å for $Pt^{II}-Tl^I$,[4] 2.70−2.71 Å for $Pt^{II}-Tl^{II}$,[5] and 2.60−2.64 Å for $Pt^{II}-Tl^{III}$ complexes,[7] depending on the formal oxidation states of the platinum and thallium atoms. The coordination number of the thallium atom is 4, and the geometry around the Tl atom may be described as a distorted tetrahedron, similarly as in the Au−Tl polymeric complex.[20] The Tl−O bond distances are 2.630(8) and 2.824(9) Å, being comparable to those in other complexes (2.17−2.86 Å),[4e,14,21] but significantly longer than the sum of the covalent radii (2.21 Å), indicating very weak Tl−O interaction.

The structure of compound **10** is depicted in Figure 2. The most striking feature of **10** differing from **8** is that the Pt−Tl chains run along 3_1 screw axes to give a helical motif. The helical pitch Pt_6Tl_6 is ∼34.38 Å. Each Pt atom links its two adjacent Tl(I) ions via both the Pt−Tl interaction and its two amidate ligands. The Pt−Tl distances are around 3.0 Å. The Pt−Tl−Pt and the Tl−Pt−Tl angles are comparable to those in **8**. The Tl−Pt−Tl is nearly linear, whereas Pt−Tl−Pt exhibits a bent geometry, similar to those in other M−Tl−M compounds.[4e,21] Another structural feature of the polymers is that the CNO units of the amidate ligands are all twisted with respect to the Pt−Tl vector, whereas the CNO units are roughly coplanar with the Pt−M axis in a number of amidate-bridged dimeric (M = Pt and Pd)[16a] and trimeric complexes (M = Mn, Fe, Co, Ni, and Cu).[16b]

By warming the aqueous solution of $[Pt(NH_3)_2(NHCO^tBu)_2]$ and $TlNO_3$ at 50 °C for 10 min and subsequently cooling the resulted colorless solution, new yellow crystals of compound **11** differing from **8** were obtained. The X-ray diffraction analysis shows that complex **11** consists of linear chains the same as those of **10**, and the chains stack to generate a trigonal architecture (space group $P3_1$).

Attempts to prepare ladderlike or gridlike coordination materials by linking the thallium ions through bipyridyl ligands such as pyrazine, 2,2′-bipy, and 4,4′-bipy were not successful. In the presence of platinum species, the thallium(I) ion shows no reactivity with the nitrogen ligands. Although Tl^+ is a large ion, it often shows exceedingly low coordination numbers in geometries, which leaves a large part of the coordination sphere seemingly unoccupied.[22] The

(20) Wang, S.; Garzón, G.; King, C.; Wang, J.; Fackler, J. P., Jr. *Inorg. Chem.* **1989**, *28*, 4623.
(21) (a) Balch, A. L.; Neve, F.; Olmstead, M. M. *J. Am. Chem. Soc.* **1991**, *113*, 2995. (b) Balch, A. L.; Nagle, J. K.; Olmstead, M. M.; Reedy, P. E., Jr. *J. Am Chem. Soc.* **1987**, *109*, 4123.

Chart 2. Schematic Representation of the Coordination Configuration of Thallium(I)

inertness of thallium centers to nitrogen ligands is ascribed to the existence of lone-pair $6s^2$ electrons, which decrease the electrophilicity of the Tl(I) ion. However, the new compound **12** was obtained in the presence of the nitrogen ligand. Complex **12** crystallizes in the achiral space group of $P2_1/n$, which has a basically similar structure to that of **11**. The helicity of these platinum−thallium(I) coordination polymers may be deduced from the absolute configuration of the thallium(I) centers shown in Chart 2. When all thallium centers have the same single absolute configuration, Δ or Λ, a P or M helical arrangement of strands would result, respectively. When the thallium(I) centers possess both absolute configurations, no helicity is generated, but it leads to a centrosymmetric molecule.

The fast atom bombardment (FAB) mass spectra of **8**−**11** show that the Pt(II)−Tl(I) unit remains intact in the gas phase. The spectrum of **9** shows peaks corresponding to $[\{Pt(NH_3)_2(NHCO^tBu)_2\}_2Tl_2(ClO_4) - H]^+$, $[\{Pt(NH_3)_2(NHCO^tBu)_2\}_2Tl - H]^+$, $[Pt(NH_3)_2(NHCO^tBu)_2Tl + H]^+$, $[Pt(NH_3)_2(NHCO^tBu)_2 + H]^+$, and the Tl^+ ion, and the binding of perchlorate was observed in the spectrum. The peak at 632.8 assigned to $[Pt(NH_3)_2(NHCO^tBu)_2Tl]^+$ is the most intense one, which clearly demonstrates that the amidate-supported dinuclear units are stable. The mass peaks at 615.79 and 598.79, corresponding to $[Pt(NH_3)_2(NHCO^tBu)_2Tl - NH_3]^+$ and $[Pt(NH_3)_2(NHCO^tBu)_2Tl - 2NH_3]^+$, indicate that NH_3 loss is preferred over Tl ion dissociation. A peak at 858.9 corresponding to $[Pt(NH_3)_2(NHCO^tBu)_2]_2$ was also observed. The FAB mass spectra of **8**−**11** are essentially the same.

Reactions of $[Pt(EtNH_2)_2(NHCO^tBu)_2]$ with Tl(I) Ions. The trinuclear complexes $[\{Pt(EtNH_2)_2(NHCO^tBu)_2\}_2Tl]X$ ($X = NO_3^-$, ClO_4^-, and PF_6^-) are the sole isolated species in the reactions of $[Pt(EtNH_2)_2(NHCO^tBu)_2]$ with Tl(I) ions; Tl^+ is available in large excess. Probably, the steric hindrance of the ethyl groups prevents further aggregation of the compound to coordination polymers.

The structure of **13** is shown in Figure 3. The two platinum units are bonded to the central Tl(I) ion via Pt−Tl bonds and two amidate ligands. Only two of the four amidate ligands are coordinated to the Tl(I) ion with two nearly identical Tl−O bond distances. This is in contrast to those of **8**−**12** in which one of the Tl−O bonds is significantly longer than the other. The Pt−Tl separations are shorter than 3.085(1) Å in the closely related Pt_2Tl complex *cis*-$[(NH_3)_2Pt(1\text{-MeT})_2Tl(1\text{-MeT})_2Pt(NH_3)_2](NO_3)\cdot 7H_2O$ (1-MeT = 1-methylthyminato).[4e] The Pt−Tl−Pt angle is also bent similarly to that of the 1-MeT-bridged trimeric compounds [136.7(1) Å].

(22) (a) Janiak, C. *Coord. Chem. Rev.* **1997**, *163*, 107. (b) Wiesbrock, F.; Schmidbaur, H. *J. Am. Chem. Soc.* **2003**, *125*, 3622.

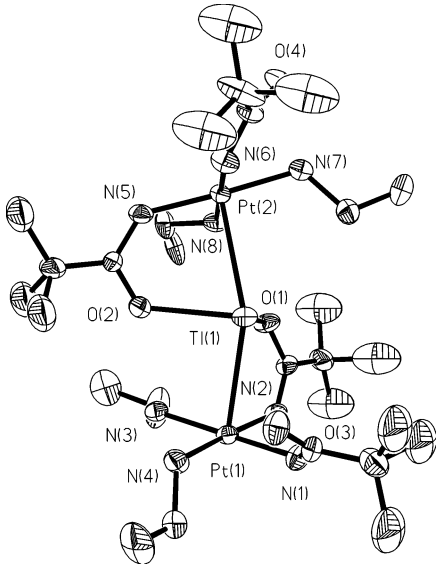

Figure 3. Molecular structure of the trinuclear cation of $[\{Pt(EtNH_2)_2(NHCO^tBu)_2\}_2Tl]^+$ (**13**). Selected bond distances (Å) and angles (deg): Pt(1)−Tl(1) 2.984(1), Pt(2)−Tl(1) 3.081(1), Pt(1)−Tl(1)−Pt(2) 140.52(2).

Reactions of $[Pt(DACH)(NHCOR)_2]$ (R = *t*Bu, CH_3) with Tl(I) Ions. Reaction of $[Pt(DACH)(NHCO^tBu)_2]$ and $TlNO_3$ yielded a trinuclear complex as a white solid even in the presence of an excess of $TlNO_3$. The compound cocrystallizes with the parent platinum complex and is formulated as $[\{Pt(DACH)(\mu\text{-}NHCO^tBu)(NHCO^tBu)\}Tl_2](NO_3)\cdot[Pt(DACH)(NHCO^tBu)_2]$ (**14**). Whereas, in the presence of $NaClO_4$ or $NaPF_6$, $[Pt(DACH)(NHCO^tBu)_2]$ gave coordination polymers of the formula $[\{Pt(DACH)(\mu\text{-}NHCO^tBu)_2\}_2Tl_2]X_2$ ($X = ClO_4^-$, **15**; PF_6^-, **16**) as yellow crystals, the reactions of $[Pt(DACH)(NHCOCH_3)_2]$ with Tl^+ always yielded the yellow coordination polymers $[\{Pt(DACH)(NHCOCH_3)_2\}_2Tl_2]X_2$ (**X** = NO_3^-, **17**; ClO_4^-, **18**; PF_6^-, **19**) with the same structures as those of **15** and **16** regardless of the counteranion, probably because of the smaller steric hindrance of acetamidate than that of pivalamidate ligands.

The structures of the cations of **15**−**19** are essentially the same; thus, only the structure of **15** is shown in Figure 4. These compounds crystallize in the same chiral space group $P2_1$, and their dimensions and symmetries within the cation $[\{Pt(DACH)(\mu\text{-}NHCOR')_2\}_2Tl_2]^{2+}$ are also similar. The polymers adopt a helical structure in the solid state. The helices are generated around the crystallographic 2_1 screw axis, and each coil of the helix contains two $[Pt(DACH)(\mu\text{-}NHCOR)_2]$ units and two Tl^+ ions. The distances between the coils corresponding to the unit cell length are ca. 22.6 Å. The extended chains of **15** are comprised of two slightly shorter Pt−Tl bonds and two longer Pt−Tl bonds (the difference between them is 0.05−0.07 Å, 50 times that of the deviation). Each pair of long and short Pt−Tl bonds is alternatively arranged. The Pt−Tl−Pt angles of **15** are around 150°, whereas the Tl−Pt−Tl angles are around 170°.

The bent Pt−Tl−Pt geometry is normally adopted in Pt(II)−Tl(I)−Pt(II) complexes, and the presence of a stereochemically active $6s^2$ thallium inert lone pair was used to explain the metal disposition. Because of the presence of the $6s^2$ electrons, the amidate oxygen atoms are loosely

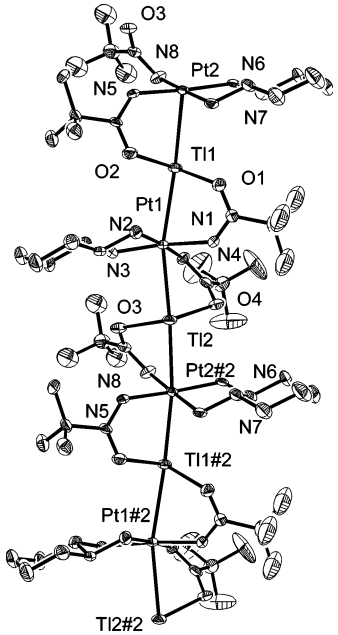

Figure 4. Asymmetric unit of the one-dimensional helical structure of complex $[\{Pt(DACH)(\mu\text{-}NHCO^tBu)_2\}_2Tl_2]^{2+}$ (**15**). Selected bond distances (Å) and angles (deg): Pt1−Tl2 2.9185(12), Pt1−Tl1 2.9914(12), Pt2−Tl2 2.9354(11), Pt2−Tl1 2.9884(12), Tl2−Pt1−Tl1 165.16(2), Tl2#1−Pt2−Tl1 171.928(17), Pt2−Tl1−Pt1 153.21(2), Pt1−Tl2−Pt2#2 144.52(3). Symmetry transformations used to generate equivalent atoms: #1 $x-1, y, z$; #2 $x+1, y, z$.

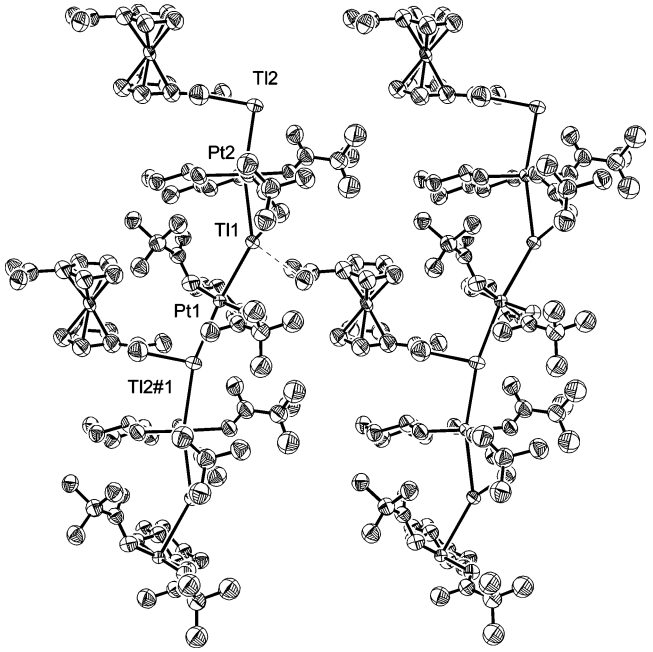

Figure 5. Perspective drawing (30% thermal ellipsoids) of the asymmetric unit in complex $[\{Pt(DACH)(NHCO^tBu)_2\}_2\{Fe(CpCO_2Tl)_2\}]$ (**20**). Selected bond distances (Å) and angles (deg): Pt1−Tl1 3.030(2), Pt1−Tl2#1 3.048(2), Pt2−Tl1 3.066(2), Pt2−Tl2 3.111(2), Pt1−Tl1−Pt2 143.93(5), Pt1−Tl2#1−Pt2#1 157.87(5), Tl1−Pt1−Tl2#1 165.55(6), Tl1−Pt2−Tl2 162.34(5).

coordinated. The geometry about the thallium ion can be viewed as a distorted trigonal bipyramid. The amidate oxygen atoms and the nonbonding lone pair are located in the equatorial plane, and two platinum atoms are at the apical positions. This coordination geometry makes the NCO units of the amidate ligands twisted, which is reflected by the large Pt−N−C−O and Tl−O−C−N torsion angles. For instance, the Pt−N−C−O angles are 8−18°, and the Tl−O−C−N angles are 23−37°. For comparison, the corresponding torsion angles of Pt−M−Pt (M = Mn, Fe, Ni, Cu, and Co) complexes are normally smaller than 5°.[16b]

Reaction of [Pt(DACH)(NHCO^{t}Bu)$_2$] with Dithallium 1,1′-Ferrocenyldicarboxylate. Dicarboxylate anions have been widely employed to construct porous metal−organic frameworks and discrete nanometer-sized functional materials.[23] Although thallium ions often show low coordination numbers in the present platinum−thallium complexes, the coordination number and coordination geometry of the thallium ion is flexible in the cases where thallium is coordinated by the hard oxygen atoms of the carboxylate groups.[21] Thus, dicarboxylate groups afford the possibility to link the Pt−Tl chains into one-dimensional ladder or two-dimensional gridlike frameworks.

The anion 1,1′-ferrocenyldicarboxylate is a suitable bridging ligand and would be able to link the platinum−thallium chains. The compound **20** was isolated as red crystals from the reaction of [Pt(DACH)(NHCO^{t}Bu)$_2$] and dithallium 1,1′-ferrocenyldicarboxylate in H_2O and acetone. A two-dimensional structure was realized in compound **20**. Crystals of compound **20** are monoclinic with a chiral space group

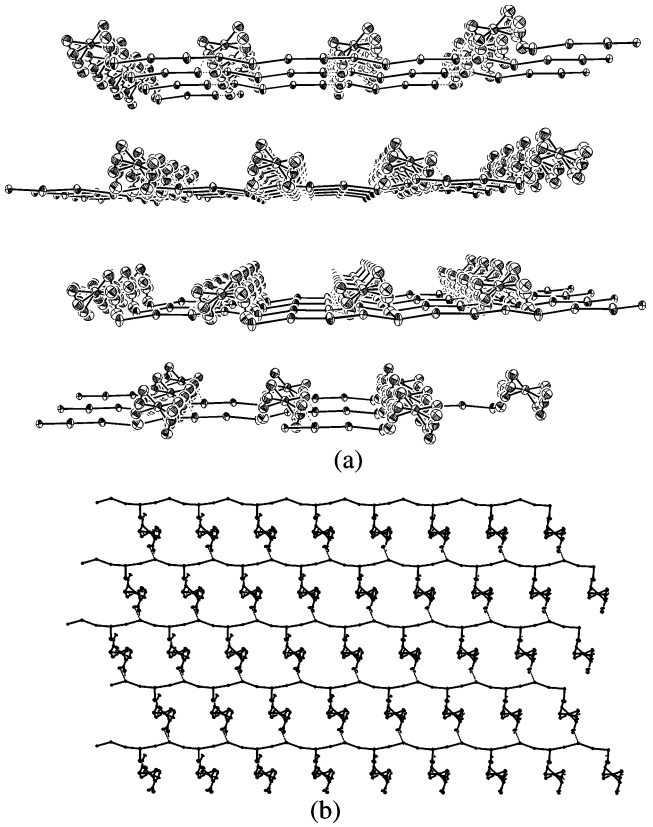

Figure 6. (a) Layered structure of $[\{Pt(DACH)(NHCO^tBu)_2\}_2\{Fe(CpCO_2Tl)_2\}]$ (**20**). The atoms of amine and amidate ligands have been removed for clarity. (b) The gridlike 2-dimensional structure.

(23) (a) Cotton, F. A.; Lin, C.; Murillo, C. A. *Inorg. Chem.* **2001**, *40*, 478. (b) Abourahma, H.; Bodwell, G. J.; Lu, J.; Moulton, B.; Pottie, I. R.; Walsh, R. B.; Zaworotko, M. J. *Cryst. Growth Des.* **2003**, *3*, 513. (c) Liu, Y.-H.; Lu, Y.-L.; Wu, H.-C.; Wang, J.-C.; Lu, K.-L. *Inorg. Chem.* **2002**, *41*, 2592.

Table 2. Luminescence Data of Compounds **8**−**10** and **13**−**19** in the Solid State

compound	298 K		77 K	
	λ_{max} (nm)	τ (ns)	λ (nm)	τ (ns)
$[Pt(NH_3)_2(NHCO^tBu)_2Tl](NO_3)$ (**8**)			477	484
$[Pt(NH_3)_2(NHCO^tBu)_2Tl](ClO_4)$ (**9**)			492	112, 567
$[\{Pt(NH_3)_2(NHCO^tBu)\}_2Tl_2](PF_6)_2$ (**10**)			470	131,561
$[\{Pt(EtNH_2)_2(NHCO^tBu)_2\}_2Tl](PF_6)$ (**13**)			481	239
$[\{Pt(DACH)(NHCO^tBu)(NHCO^tBu)\}_2Tl](NO_3)\cdot[Pt(DACH)(NHCO^tBu)_2]$ (**14**)			476	327, 1237
$[\{Pt(DACH)(NHCO^tBu)_2\}_2Tl_2](ClO_4)_2$ (**15**)	520	21, 91	544	923
$[\{Pt(DACH)(NHCO^tBu)_2\}_2Tl_2](PF_6)_2$ (**16**)	493	15, 43	510	87, 539
$[\{Pt(DACH)(NHCOCH_3)_2\}_2Tl_2](ClO_4)_2$ (**17**)	469	30, 95	485	81, 549
$[\{Pt(DACH)(NHCOCH_3)_2\}_2Tl_2](ClO_4)_2$ (**18**)	467	19, 80	481	158, 567
$[\{Pt(DACH)(NHCO^tBu)_2\}_2\{Fe(CpCO_2Tl)_2\}]$ (**19**)	474	116, 238	487	236, 863

$P2_1$ (Figure 5). The Pt−Tl bond distances of the thallium coordinated to 1,1′-ferrocenyldicarboxylate are somewhat longer than the others. Each carboxylate group of 1,1′-ferrocenyldicarboxylate is monocoordinated to thallium with a Tl−O distance of 2.35(5) Å. The Pt−Tl−Pt−Tl unit constitutes an extended helical chain along the crystallographic *b* axis. The infinite helical chain of compound **20** can be viewed as a repeated alternate stacking of the trimetallic unit $[\{Pt(DACH)_2(NHCO^tBu)_2\}_2Tl]^+$ and $[Fe(CpCO_2)_2Tl]^-$ via Pt−Tl bonds.

The neighboring helical chains are linked by 1,1′-ferrocenyldicarboxylate anions to yield the two-dimensional supramolecular gridlike structure (Figure 6). The grids stack and form "stacked layers". The stacking exhibited by the grids forms microchannels that run approximately perpendicular to the layers and water molecules filled between layers.

Solid-State Emission Spectroscopy. The luminescence spectra have been recorded at 77 and 298 K, and the results are summarized in Table 2. The coordination polymers derived from $[Pt(NH_3)_2(NHCO^tBu)_2]$ exhibit intense luminescence in the solid state at 77 K, whereas they are nonemissive at room temperature. The luminescence spectrum of **8** is very sharp and structureless with the maximum at 477 nm and full width at half-maximum of 1280 cm^{-1}, when irradiated at 400 nm. The spectral features as well as the emission lifetime of 484 ns clearly indicate that the luminescence originates from the triplet metal-centered state of the complex with the Pt(II)−Tl(I) bond and are comparable to those of $Tl_2Pt(CN)_4$.[4a,24] The emission of **9** occurs at 492 nm, while that of **10** is found at 470 nm. The emission of **9** and **10** displays biexponential kinetics ($\tau_1 = 112$ ns, $\tau_2 = 567$ ns for **9**; $\tau_1 = 131$, $\tau_2 = 561$ ns for **10**). The small difference in the emission maximum may result from the variation of the counteranions.

Emission was not observed for trinuclear compounds **13** and **14** in the solid state at room temperature, whereas on cooling of the colorless crystals to 77 K, intense emission was observed at 481 and 476 nm, respectively. However, the polymeric platinum−thallium complexes **15**−**19**, derived from $[Pt(DACH)(NHCOR)_2]$ (R = ^{t}Bu, CH_3) luminesce both at room temperature and at 77 K. At 298 K, complexes **15**−**19** emit with the maximum range of 467−520 nm, whereas at 77 K, they emit with the maximum range of 481−544 nm. The red shift observed for these complexes with a decrease of temperature has been found in some luminescent materials[25] and is related to a thermal contraction that leads to a reduction in the metal−metal distances along the chain, reducing the band gap energy. Compounds **17**−**19** emit at higher energies compared to compounds **15** and **16**, which is reasonably understood when taking into account the shorter Pt−Tl bonds within the chains of **15** and **16** than those of **17**−**19**. The long lifetime of the emissive states and the large Stokes shifts illustrate the triplet origin. The triplet state could be ascribed to the increased electronic delocalization over the platinum−thallium chain because of the more intense Pt−Tl interactions compared to the known simple Pt−Tl complexes.

The emission from d^8-s^2 mixed metal complexes is well-established. The d^8-s^2 bond interaction is a known reason for the photoluminescence in Pt−Tl complexes.[26] Significant overlap between the filled $5d_z^2$ orbitals of platinum and the empty 6p orbitals of thallium is responsible for the emissive behaviors. The ground-state Pt−Tl interaction is stabilized by the mixing of the filled $5d_z^2$ level on Pt(II) and the filled 6s level on Tl(I) with the empty $6p_z$ level on both metals. It is noted that the emission energy for the chain compounds is lower than that for the trinuclear complexes. This is obviously due to the expected lower band gap energy in the extended-chain species in the solid state than that for oligomers.

Summary

Self-assembly from simple molecules or ions is an optimum synthetic method for generating supramolecules with optical or optoelectronic properties. The bimetallic platinum−thallium complexes are readily synthesized by the reaction of $[Pt(RNH_2)_2(NHCO^tBu)_2]$ and thallium(I) salts. These compounds are rare examples of one- and two-dimensional chain materials containing Pt−Tl metallic backbones. Generally, the platinum−thallium interactions between simple platinum precursors and Tl(I) ions lead to

(24) Dolg, M.; Pyykko, P.; Runeberg, N. *Inorg. Chem.* **1996**, *35*, 7450.

(25) (a) Fernández, E. J.; Gimeno, M. C.; Laguna, A.; López-de-Luzuriaga, J. M.; Monge, M.; Pyykkö, P.; Sundholm, D. *J. Am. Chem. Soc.* **2000**, *122*, 7287. (b) Fernández, E. J.; Jones, P. G.; Laguna, A.; López-de-Luzuriaga, J. M.; Monge, M.; Pérez, J.; Olmos, M. E. *Inorg. Chem.* **2002**, *41*, 1056.

(26) (a) Clodfelter, S. A.; Doede, T. M.; Brennan, B. A.; Nagle, J. K.; Bender, D. P.; Turner, W. A.; LaPunzina, P. M. *J. Am. Chem. Soc.* **1994**, *116*, 11379. (b) Wissbart, B.; Balch, A. L.; Tinti, D. S. *Inorg. Chem.* **1993**, *32*, 2096.

Chart 3

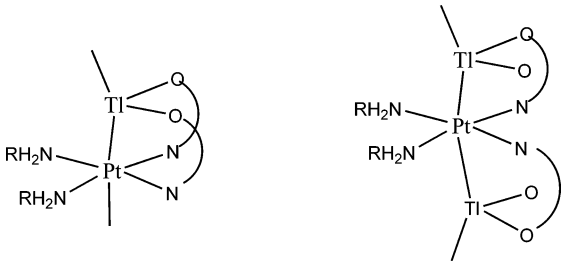

dimers or trimers. Obviously, the functionality of the amidate ligands in the present system plays an important role in the self-aggregation of the two units into extended structures. These coordination polymers are comprised of helical or zigzag alternate platinum and thallium chains in which the two metals are singly or doubly bridged by amidate ligands, as shown in Chart 3.

The luminescence observed from these solids arises from the association of $[Pt(RNH_2)_2(NHCO^tBu)_2]$ and Tl^+ through metallophilic interactions. The emissive energy is sensitive to variation of the substituents, counteranions, and temperature. The compounds may readily dissolve in hot water or H_2O and acetone with dissociation, but they can be easily regenerated by evaporation of the solvent and the linearly arranged Pt−Tl backbone maintained. This feature and the luminescence property make these compounds suitable candidates of stable, water-soluble, solution-processible functional materials for potential sensor applications.

Acknowledgment. W.C. thanks the National Science Foundation of China and Zhejiang Provincial Science Foundation for support.

Supporting Information Available: The crystallographic data and structures of compounds **9**, **11**, **12**, and **14**−**16** and X-ray crystallographic files in CIF format for compounds **8**−**10**, **13**−**17**, and **20**. This material is available free of charge via the Internet at http://pubs.acs.org.

IC051932C